

# Amelioration of Titanium Dioxide nanoparticles induced injury on the cerebellum of the adult mice by a hydromethanolic root extract of *Withania Somnifera*

Original  
Article

*Nermeen Mohammed Faheem and Amgad Gaber Elsaid*

*Department of Anatomy and Embryology, Faculty of Medicine, Ain Shams University, Egypt*

## ABSTRACT

**Introduction:** Titanium Dioxide (TiO<sub>2</sub>) nanoparticles have potential risks to human health. They were able to enter brain to be detected in the cerebral cortex, cerebellum and hippocampus. *Withania somnifera* (WS) improve rotenone induced damage in cerebellum.

**Aim of the work:** To study the effects of oral administration of TiO<sub>2</sub> nanoparticles on the cerebellum and the protective role of hydromethanolic root extract of WS (Egyptian Ashwaghandha).

**Material and Methods:** Seventy five adult male albino mice were divided into five groups (N=15): group 1 (control), group 2 (gum acacia group), and group 3 (WS root extract group) received orally hydromethanolic WS root extract (500 mg/kg) once daily, group 4 (TiO<sub>2</sub> nanoparticles group) received orally TiO<sub>2</sub> nanoparticles (150 mg/ Kg), dissolved in gum acacia solution once daily, group 5 (TiO<sub>2</sub> nanoparticles + WS root extract group). After sixty days, Sections from the cerebellum were prepared and stained with HandE, Cresyl violet stain as well as Immunohistological stains for nNOS, iNOS, eNOS and GFAP. Morphometrical and statistical analyses were performed.

**Results:** In TiO<sub>2</sub> nanoparticles group, cerebellum showed disrupted purkinje cells with marked degenerative changes, decreased Nissl granules in Purkinje cells, vacuolations in all layers of the cerebellar cortex and dilated congested capillaries in white matter. The number of the Purkinje cell were decreased while GFAP positive astrocytes were increased. Decreased nNOS immunostaining in cortical layers, while the iNOS immunostaining increased and increased eNOS immunostaining in capillary endothelial cells were detected. Administration of the hydromethanolic WS root extract improved the altered cerebellar morphology with significant statistical improvement in purkinje cell and astrocyte count.

**Conclusion:** TiO<sub>2</sub> nanoparticles oral administration induced toxic effects and WS contains active ingredients that counteract these effects.

**Received:** 05 October 2015, **Accepted:** 23 July 2018

**Key Words:** Cerebellum, mice, tiO<sub>2</sub> nanoparticles, withania somnifera.

**Corresponding Author:** Nermeen Mohammed Faheem, MD, Department of Anatomy and Embryology, Faculty of Medicine, Ain Shams University, Egypt, **Tel.:** +20 1003374746, **E-mail:** nermeenfaheem@yahoo.com

**ISSN:** 1110-0559, Vol. 41, No. 4

## INTRODUCTION

Titanium (Ti) is widely distributed around the world. It is the ninth most abundant element in the earth's crust. Ti is not found as a pure metal in nature due to its high affinity for oxygen and other elements. Titanium Dioxide (TiO<sub>2</sub>) is a natural derivative of the Ti<sup>[1]</sup>.

Nanoparticles are a class of organic or inorganic substances with the size (1–100 nm). They can be generated through both natural (e.g., volcano eruption) or produced daily by human activities (automobile exhaust gases or emissions of power plants) or engineered for industrial or medical purposes<sup>[2]</sup>.

TiO<sub>2</sub> is in the top five nanoparticles used in consumer products<sup>[3]</sup>. Oral route has a potential exposure route for general population due to TiO<sub>2</sub> frequently used as a "whitening" pigment in tooth paste, in tableted drug products, in dairy based products as cheese, chocolate and

milk powder and in bread flour. Also, TiO<sub>2</sub> is therapeutically used in sunscreens and cosmetic creams<sup>[4]</sup>.

The distinct properties of TiO<sub>2</sub> nanoparticles, such as small size, high number per given mass, increased surface area per unit mass, aggregation and marked reactivity may cause harmful effects to human health and the environment<sup>[5]</sup>.

TiO<sub>2</sub> nanoparticles were able to enter the brain to be detected after 10 days of exposure in many areas of the brain, including the cerebral cortex, cerebellum and hippocampus and produced histopathological changes in the CA1 region of the hippocampus<sup>[6]</sup>.

Nanoparticulate TiO<sub>2</sub> significantly increased the activities of nitric oxide (NO) level in the mouse brain also, the regulation of NO plays a role in nanotoxicology<sup>[7]</sup>.

The cerebellum forms the highest levels of NO within

the nervous system<sup>[8]</sup>. This high levels of NO may indicate that cerebellum is more susceptible to oxidative stress. Oxidative stress markers included inducible nitric oxide synthase (iNOS), neuronal NOS (nNOS) and endothelial NOS (eNOS)<sup>[9]</sup>.

Cerebellum is included in frequent aspects of motor functions including coordination, muscle tone, locomotion and posture. It also has a role in behavior, cognition, speech, psychiatric illness as well as discrimination of sensory information<sup>[10]</sup>.

Glial cells play a principal role in the development, formation, nutrition and repair of neurons. These cells also direct the axonal regeneration process. Glial fibrillary acidic protein (GFAP) is a good indicator of early pathological effects, indicated by the activation of astrocytes<sup>[11]</sup>.

Traditional medicines are usually derived from natural products as plants, minerals and organic materials<sup>[12]</sup>. *Withania somnifera* (WS), commonly known as Ginseng and Ashwagandha, is an important medicinal plant, a small, woody shrub 60–200 cm high. It is grown in India, Pakistan, Afghanistan, the Mediterranean and throughout the Middle East especially Egypt and Jordan<sup>[13]</sup>.

The roots of WS are commonly used for therapeutic purposes. The dried roots of the plant have been shown to have a useful role in the treatment of nervous and sexual dysfunction<sup>[14]</sup>.

WS is reported to be beneficial in many nervous disorders in rodents. These include stress<sup>[15]</sup> and rotenone-induced oxidative stress<sup>[16]</sup>.

Administration of WS was found to be safe and showed enhanced body posture and increased strength and stability in limb movements in elderly patients with long-term progressive degenerative cerebellar ataxia<sup>[17]</sup>.

Unfortunately, few studies have been carried out to determine effects of TiO<sub>2</sub> nanoparticles on cerebellum and natural ways for protection. So, the aim of the present study was to investigate the effect of hydromethanolic root extract of WS on cerebellum of albino mice subjected to TiO<sub>2</sub> nanoparticles.

## MATERIAL AND METHODS

### *Experimental animals:*

Seventy five healthy male mice aged two months locally bred at the animal house of Research Center and Bilharzial Research Unit, Faculty of Medicine, Ain Shams University. The mice were housed in stainless steel cages, five mice per cage. The mice were exposed to dark/light cycle and daily diet and free water access were allowed with suitable environmental conditions and good ventilation and at a temperature of 25 degrees.

### *Chemicals*

TiO<sub>2</sub> nanoparticles: It is nanopowder of 21 nm particle size and purity  $\geq 99.5\%$  trace metals basis they were

white and odorless. It is manufactured by Sigma-aldrich Chemical Company, Germany and purchased from Sigma-Egypt.

Gum acacia: It is presented in a powder form and prepared by dissolving 10 gm in 100 ml distilled water which were boiled first. It was obtained from El-Nasr Pharmaceutical Chemicals Company, Egypt.

*Withania Somnifera* (Egyptian Ashwagandha), dried roots were obtained from a local market.

Preparation of hydromethanolic WS root extract: The powdered WS roots (50g) were extracted successively with 80% methanol and 20% H<sub>2</sub>O in a soxhlet extractor for 48 h at 60°C. The solvent was evaporated to dryness at 40°C by a rotary evaporator. The powder was 5g/kg and stored at 4°C. It was dissolved in distilled water whenever needed for experiment<sup>[18]</sup>.

### *Experimental design:*

The animals were divided into five groups (n=15).

**Group1 (control group):** received 1 ml of distilled water orally through a gastric tube once daily for sixty days.

**Group2 (gum acacia group):** received 1ml of 5% gum acacia solution (solvent of TiO<sub>2</sub> nanoparticles) orally through a gastric tube once daily for sixty days.

**Group3 (WS root extract group):** received hydromethanolic WS root extract at a dose of 500 mg/kg orally through a gastric tube once daily for sixty days<sup>[18]</sup>.

**Group4 (TiO<sub>2</sub> nanoparticles group):** received TiO<sub>2</sub> nanoparticles (150 mg/ Kg)<sup>[19]</sup>, in 1 mL of 5% gum acacia solution as a solvent orally through a gastric tube once daily for sixty days<sup>[20]</sup>.

**Group5 (TiO<sub>2</sub> nanoparticles+WS root extract group):** received a TiO<sub>2</sub> nanoparticles as in group 4 with hydromethanolic WS root extract as in group 3 for sixty days.

At the end of the experiment the animals were sacrificed by high dose of ether anesthesia. The skull was opened and the cerebella were collected carefully. the cerebella were cut in parasagittal sections and fixed in 10% formaline for two more days. The specimens were prepared for paraffin blocks. Paraffin sections (5um) of cerebellar hemispheres were stained with hematoxylin and eosin stain and Cresyl fast violet stain<sup>[21]</sup>.

### *Immunohistochemical study for GFAP:*

Immunostaining was performed using the avidin-biotin peroxidase technique for localization of GFAP, and the same technique for the iNos, nNos and eNos: Paraffin sections (5um) were stained with modified avidin-biotin peroxidase technique for GFAP to demonstrate the astrocytes. Primary antibodies were obtained from (Sigma, St Louis, Missouri, USA). Sections underwent deparaffinization and hydration. Then treated with 0.01 M citrate buffer for 10

minutes to unmask antigen. Then, they were incubated in 0.3% H<sub>2</sub>O<sub>2</sub> for 30 minutes to abolish endogenous peroxidase activity before blocking with 5% horse serum for 1-2 hs. The specimens were incubated with the primary antibody (1:100 monoclonal mouse anti GFAP) at 4°C for 18-20hs. The next step was washing and incubating the slides with biotinylated secondary antibodies and then with avidinbiotin complex. Lastly, sections were counterstained with hematoxylin before mounted<sup>[22]</sup>.

### Quantitative morphometric study

The number of Purkinje cells per field was calculated. Five fields from three several sections stained by Cresyl fast violet of each rat were examined by high power lens (X400), using the image analyzer program at Faculty of Science, Azhar University. In every section, the cell that was located at the purkinje cell layer had a soma and at least a part of its nucleus in the section was counted<sup>[23]</sup>.

Also, astrocytes were counted in an area of 20,000 μm<sup>2</sup> and selected randomly in the GFAP stained sections using light microscopy at ×400 magnification.

In addition the total number of Purkinje cells in section was estimated by manual counting. Mean of nNOS and iNOS immunopositive Purkinje cells were assessed. Measurements were performed on five sections per group. In the nNOS and iNOS stained sections using light microscopy at ×400 magnification.

### Statistical analysis

The values were represented as mean ±Standard Deviation (±SD). The data were analyzed by one-way anova with post-hoc test for multiple comparisons between groups using SPSS software (SPSS Inc., Chicago, Illinois, USA). Differences were considered significant if *P* value was less than 0.05 and highly significant if *P* value was less than 0.01.

## RESULTS

### Histological results:

#### Group1: control group:

HandE-stained sections showed the central white matter with the overlying outer cortex of grey matter. The grey matter was found to be composed of three well defined layers. These layers were the outer molecular layer, the inner granular layer and the Purkinje layer in between the previous two layers (Fig. 1).

The molecular layer was formed of nerve fibers with few scattered stellate cells located superficially and basket cells in the deeper parts near Purkinje cell bodies. The Purkinje cells were uniformly arranged in one row along the outer margin of the granular layer. They showed large pyriform or flask shaped cell bodies. They displayed characteristic centrally located vesicular nuclei and apparent nucleoli. Bergmann astrocytes with pale nuclei surrounded by a pale cytoplasm were identified. They were scattered in the superficial part of the granular cell layer and in between

the Purkinje cells. The granular layer was composed of numerous, small, closely packed granular cells with dark spherical nuclei and non-cellular clear spaces in between the cells, representing the cerebellar islands (Fig. 2).

With cresyl fast violet stain, purple Nissl granules were detected in the perikarya of Purkinje cells (Fig. 3).

Group2 (Gum acacia group) and group3 (WS root extract group):

Showed the same histological appearance like control group I.

Group4 (TiO<sub>2</sub> nanoparticles group):

HandE stained sections showed that purkinje neurons disappeared completely in many areas leaving empty spaces. The granular layer was thin with many apoptotic cells having small eccentric dark nuclei and an eosinophilic cytoplasm (Fig. 4).

other sections showed abnormal arrangement of the Purkinje cells in more than one layer. Purkinje cells were displaced upwards in the molecular layer, while others were intermingling with granular cells. Their nuclei showed karyolytic changes. Many Bergmann astrocytes were identified in molecular layers and in the granular layer. Vacuolations were detected in all the layers of the cerebellar cortex (Fig. 5).

Other Purkinje cells were shrunken and having eosinophilic cytoplasm or vacuolated cytoplasm and shrunken dark stained nuclei. They were surrounded with perineural spaces with accumulation of numerous glial cells around some of them (Fig. 6).

White matter showed areas of hemorrhage and dilated congested blood vessels (Fig. 7).

Cresyl fast violet stain revealed decreased Nissl granules in Purkinje cells (Fig. 8).

#### Group5 (TiO<sub>2</sub> nanoparticles + WS root extract group):

Examination of the HandE stained sections of this group showed monolayer of Purkinje cells that most of them retained its pyriform shape and their characteristic centrally located vesicular nuclei and apparent nucleoli between the outer molecular and inner granular layers. Few affected Purkinje cells were observed with fragmented nucleus and eosinophilic cytoplasm inbetween apparently normal cells. Bergmann astrocytes were arranged in the superficial part of the granular cell layer and in between the Purkinje cells (Fig. 9).

No apparent changes were detected in molecular layer or in white matter. Few vacuolation appear in the granular layer (Fig. 10).

As regards Cresyl fast violet stain sections, slight increase in Nissl granules in the Purkinje cells as compared to TiO<sub>2</sub> nanoparticles group (Fig. 11).

### Immunohistological results:

In control animals, immunohistochemical staining for the detection of GFAP showed scattered GFAP positive astrocytes in the white matter and molecular layers (Fig. 12a). In the TiO<sub>2</sub> nanoparticles group, GFAP-positive astrocytes were greater in number, with multiple thick processes, with relatively longer processes in the white matter and the three cerebellar cortical layers (Fig. 12b). The TiO<sub>2</sub> nanoparticles group showed relatively fewer astrocytes with thin processes in the white matter, granular, Purkinje and molecular layers. (Fig. 12c).

nNOS immunostaining of control group showed positive nNOS immunoreactivity in the molecular layer in the perikarya of stellate and basket cells. The cell bodies of Purkinje cells and the granular layer also exhibit positive nNOS immunoreactivity (Fig. 13a). In the TiO<sub>2</sub> nanoparticles group, weak nNOS immunoreactivity was observed in the molecular layer, the granular layer and Purkinje cell layer (Fig. 13b). The TiO<sub>2</sub> nanoparticles + WS root extract group showed improvement in nNOS immunoreactivity in molecular, granular layer and Purkinje cell layers (Fig. 13c).

Immunohistochemical staining for iNOS revealed slight iNOS immunoreactivity in the molecular layer and granular layer. Most Purkinje cell bodies are non-immunoreactive in the control mice (Fig. 14a). In the TiO<sub>2</sub> nanoparticles group, granular cell layer shows moderate reaction in some areas while the molecular layer shows mild immunoreactivity. However, iNOS strong immunoreaction was observed in Purkinje cells (Fig. 14b). TiO<sub>2</sub> nanoparticles + WS root extract group showed mild iNOS immunoreactivity in the molecular layer and in few areas of granular layer while Purkinje cells are non-immunoreactive (Fig. 14c).

Immunohistochemical staining for the eNOS revealed negative reaction in the capillary endothelial cells (Fig. 15a). However, the TiO<sub>2</sub> nanoparticles group showed strong positive reaction in the capillary endothelial cells (Fig. 15b) while the TiO<sub>2</sub> nanoparticles + WS root extract group showed mild positive reaction (Fig. 15c).

### Statistical results:

#### A) Number of the Purkinje cells / 10000 mm<sup>2</sup> area of the Purkinje cell layer:

There was highly statistically significant difference between groups as regards the number of Purkinje cells,  $P < 0.001$ , F value = 525.9 (Anova test) (Table 1 and Histogram 1).

There was no significant statistical difference in the number of Purkinje cells between control, gum acacia and WS root extract groups.

#### B) Number of astrocytes / an area of 20 000 μm<sup>2</sup>:

There was highly statistically significant difference between groups as regards the number of astrocytes,  $P < 0.001$ , F value = 319.5 (Anova test) (Table 2 and Histogram 2).

There was no significant statistical difference in the number of astrocytes between control, gum acacia and WS root extract groups.

#### C) Number of the nNOS and iNOS positive Purkinje cells:

There was highly statistically significant difference between groups as regards the the nNOS and iNOS positive Purkinje cells,  $P < 0.001$  (Anova test) (Table 3 and Histogram 3).

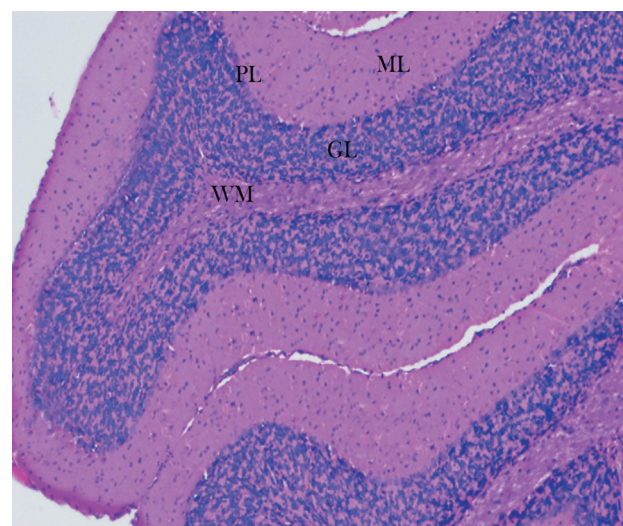


Fig. 1: A photomicrograph of a section of the cerebellum of an adult control mouse showing the different layers of the cerebellar cortex which are molecular layer (ML), Purkinje layer (PL) and granular layer (GL), as well as the white matter (WM). H and E; X 100

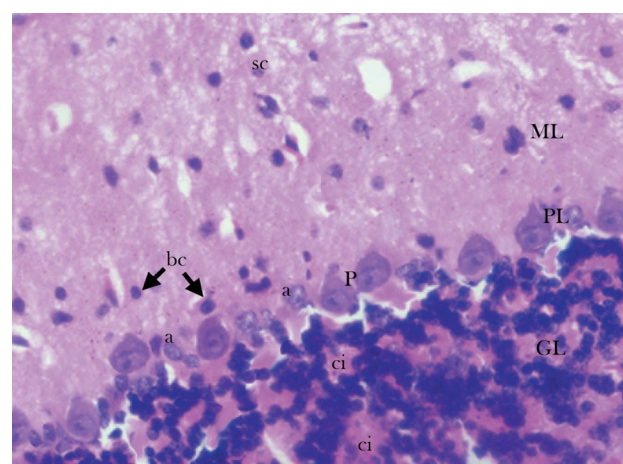
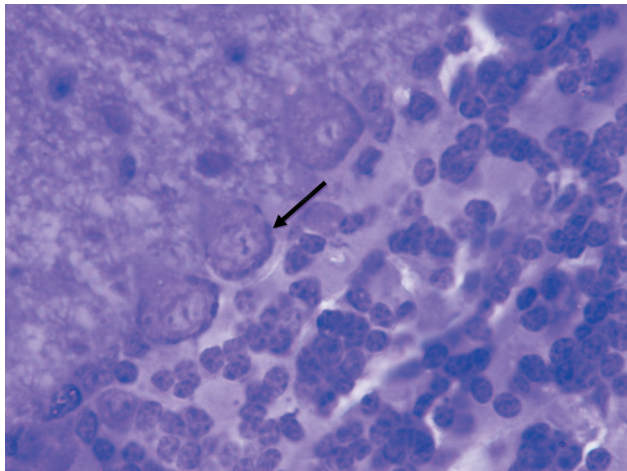
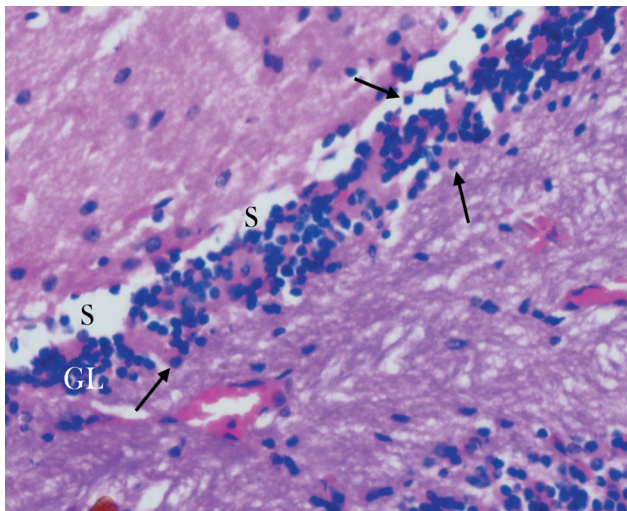


Fig. 2: A photomicrograph of a section of the cerebellum of an adult control mouse showing the molecular layer (ML) is formed of small stellate (sc) and basket (bc) cells. The Purkinje cells (P) of the middle layer (PL) The granular layer (GL). Note the presence of clear spaces cerebellar islands (ci) and Bergmann astrocytes (a). H and E; X 400



**Fig. 3:** A photomicrograph of a section of the cerebellum of an adult control mouse showing purple Nissl granules (arrow) in the perikarya of Purkinje cells. Cresyl fast violet × 1000



**Fig. 4:** A photomicrograph of a section of the cerebellum of an adult mouse of the TiO<sub>2</sub> nanoparticles group showing loss of Purkinje neurons leaving empty spaces (s).

Note the thin granular layer (GL) with many apoptotic cells having small eccentric nuclei and an eosinophilic cytoplasm (arrow). H and E; X 400

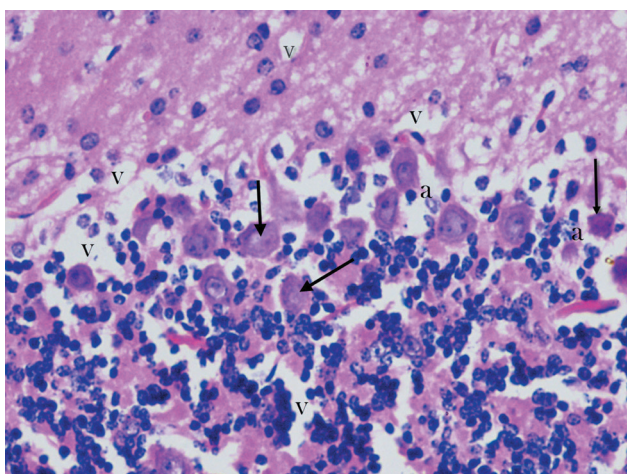


**Fig. 5:** A photomicrograph of a section of the cerebellum of an adult mouse of the TiO<sub>2</sub> nanoparticles group showing disarrangement of the Purkinje cells lineage. Some of them showed eosinophilic cytoplasm and karyolytic changes (arrow). All the layers of the cerebellar cortex showed vacuolation (v).

Note the presence of many Bergmann astrocytes (a). H and E; X 400

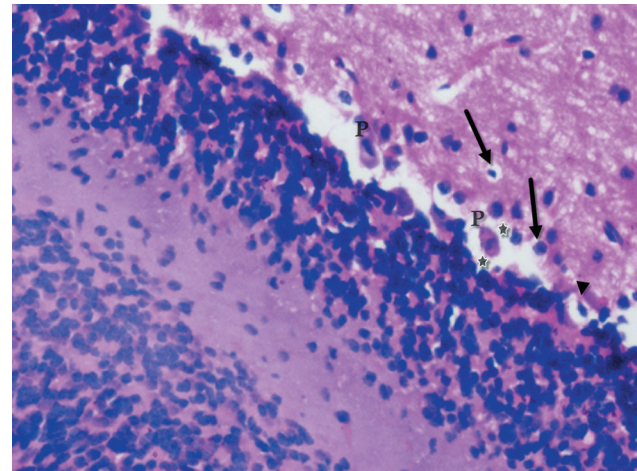


**Fig.6:** A photomicrograph of a section of the cerebellum of an adult mouse of the TiO<sub>2</sub> nanoparticles group showing halos of empty spaces (stars) and numerous glia (arrow) surround the shrunken purkinje cells (P) with eosinophilic cytoplasm and dark stained shrunken nuclei. Note the purkinje cell (arrow head) with completely vacuolated cytoplasm and dark stained shrunken nuclei. H and E; X 400

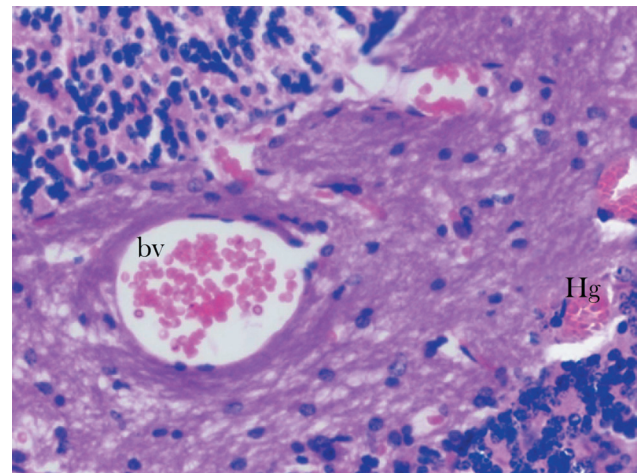


**Fig. 7:** A photomicrograph of a section of the cerebellum of an adult mouse of the TiO<sub>2</sub> nanoparticles group showing dilated congested blood vessel (bv) in white matter. Note the hemorrhage (Hg) in the white matter. H and E; X 400

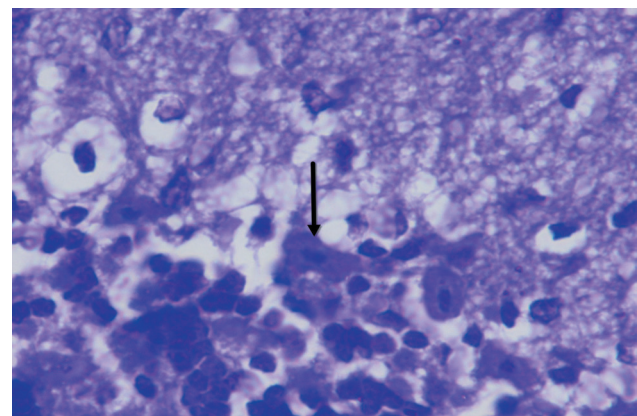


**Fig. 8:** A photomicrograph of a section of the cerebellum of an adult mouse of the TiO<sub>2</sub> nanoparticles group showing decreased purple Nissl granules in the perikarya of Purkinje cells (arrow). Cresyl fast violet × 1000

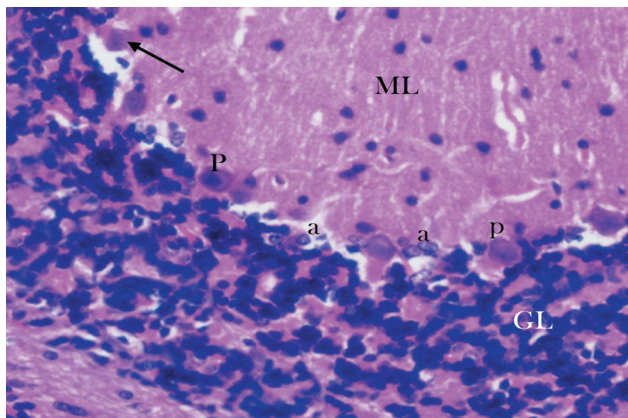


**Fig. 9:** A photomicrograph of a section of the cerebellum of an adult mouse of TiO<sub>2</sub> nanoparticles + WS root extract group showing monolayer of Purkinje cells (P) in between the molecular (ML) and granular layer (GL). Note the presence of Bergmann astrocytes (a) and Purkinje cells with fragmented nucleus and eosinophilic cytoplasm (arrow). H and E; X 400

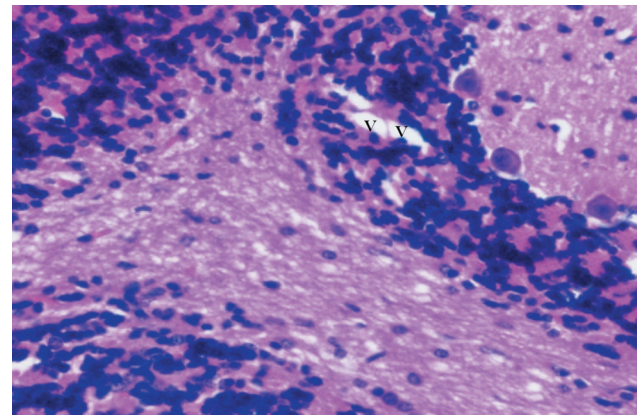


**Fig. 10:** A photomicrograph of a section of the cerebellum of an adult mouse of TiO<sub>2</sub> nanoparticles + WS root extract group showing some vacuolation (v) in the granular layer. H and E; X 400

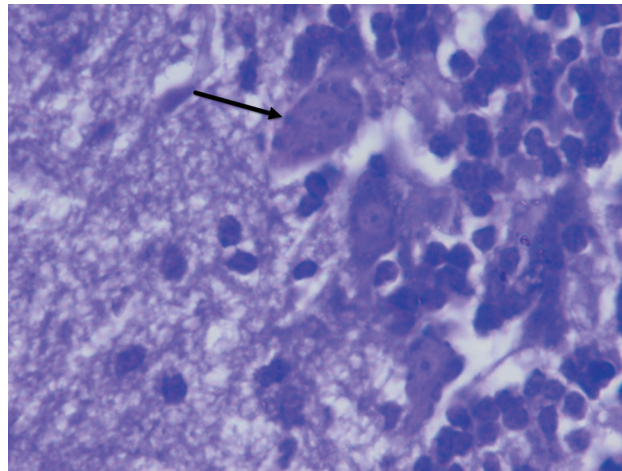


**Fig. 11:** A photomicrograph of a section of the cerebellum of an adult mouse of the TiO<sub>2</sub> nanoparticles + WS root extract group showing slight increase in Nissl granules in the perikarya of Purkinje cells. (arrow) Cresyl fast violet × 1000.

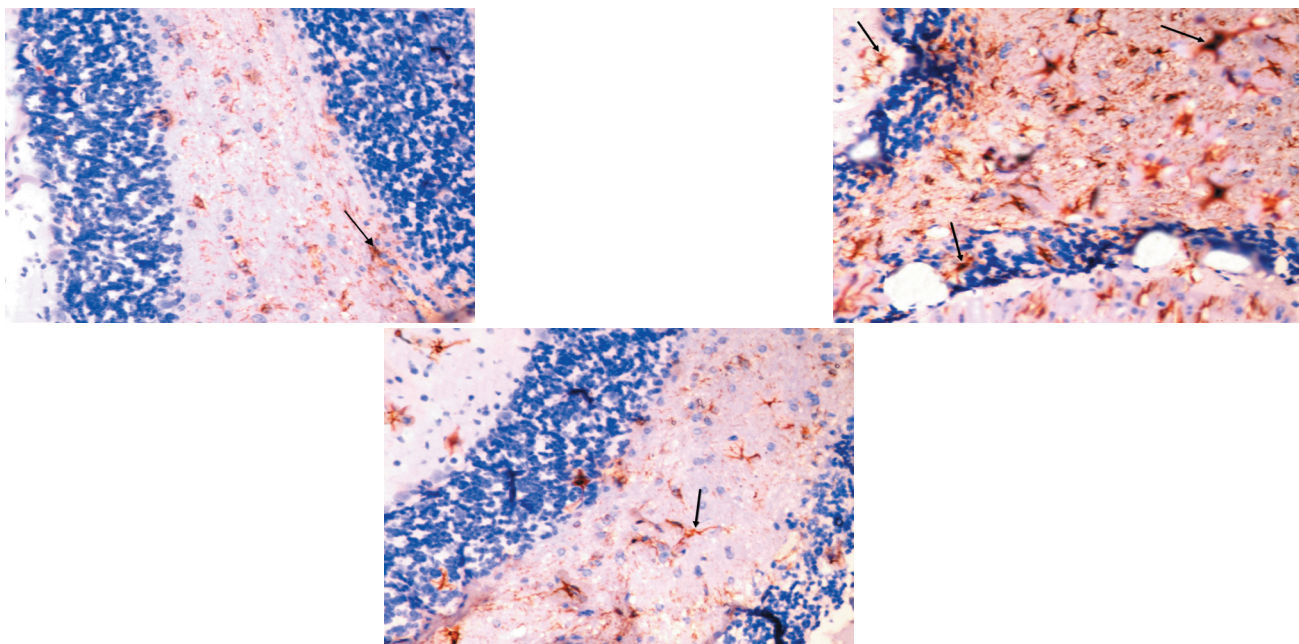


**Fig. 12:** Immunohistochemical staining for the demonstration of GFAP in the cerebellum of: a) an adult control mouse showing scattered positive astrocytes (arrows) in the white matter and granular layer. b) an adult mouse of the TiO<sub>2</sub> nanoparticles group showing GFAP-positive astrocytes; they were greater in number, with multiple thick processes, with relatively longer processes (arrows) in the white matter, granular, Purkinje and molecular layers. C) an adult mouse of the TiO<sub>2</sub> nanoparticles + WS root extract group showing relatively fewer astrocytes with thin processes in the white matter, granular, Purkinje and molecular layers. GFAP, × 400

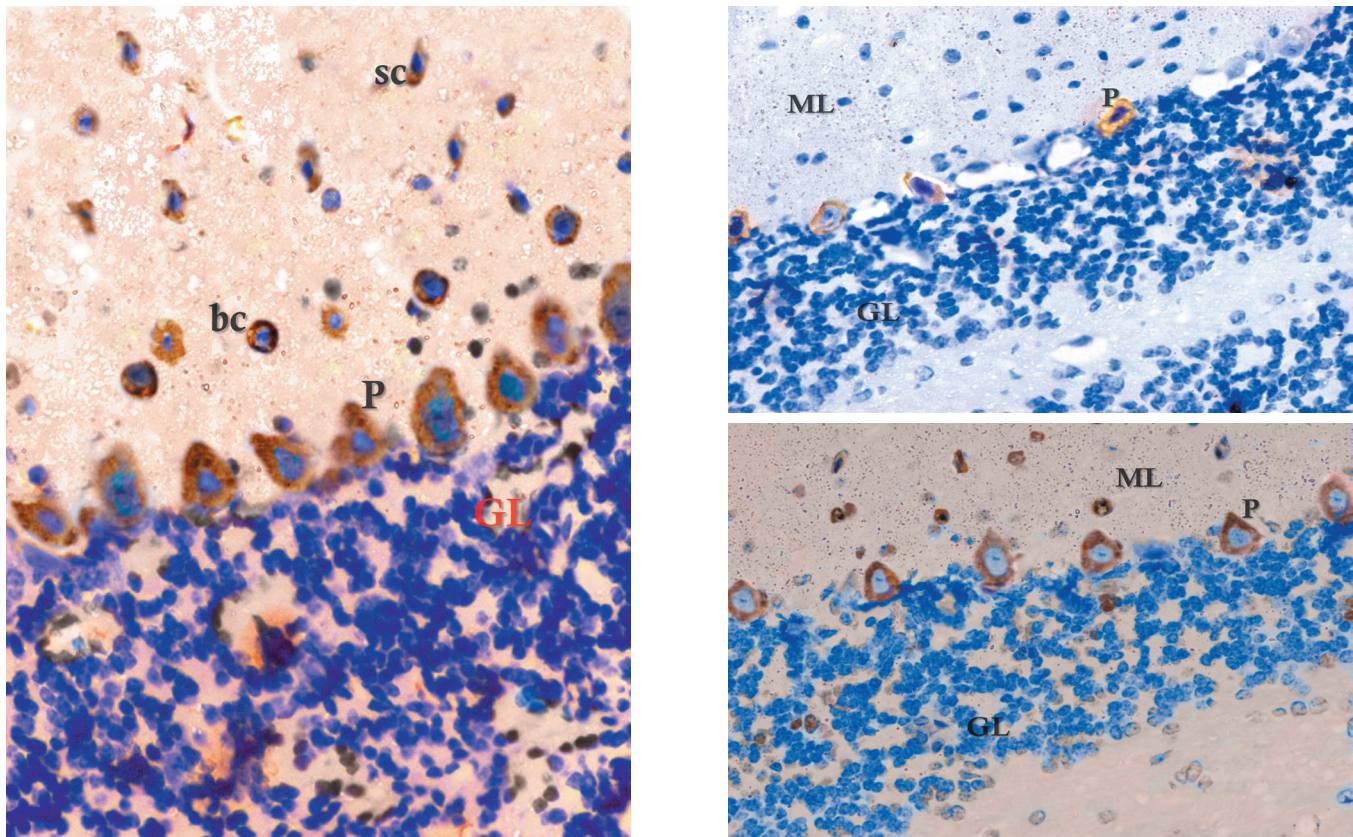


**Fig.13:** Immunohistochemical staining for the nNOS in the cerebellum of: a) an adult control mouse showing nNOS immunoreactivity in the molecular layer in the perikarya of stellate (sc) and basket (bc) cells. The cell bodies of Purkinje cells (P) and the granular layer (GL) also exhibit nNOS immunoreactivity. b) an adult mouse of the TiO<sub>2</sub> nanoparticles group showing weak nNOS immunoreactivity in the molecular layer (ML), the granular layer (GL) and Purkinje cell (P) layer. c) an adult mouse of the TiO<sub>2</sub> nanoparticles + WS root extract group showing increased nNOS immunoreactivity in the molecular layer (ML), granular layer (GL) and Purkinje cells (P). nNOS, × 400

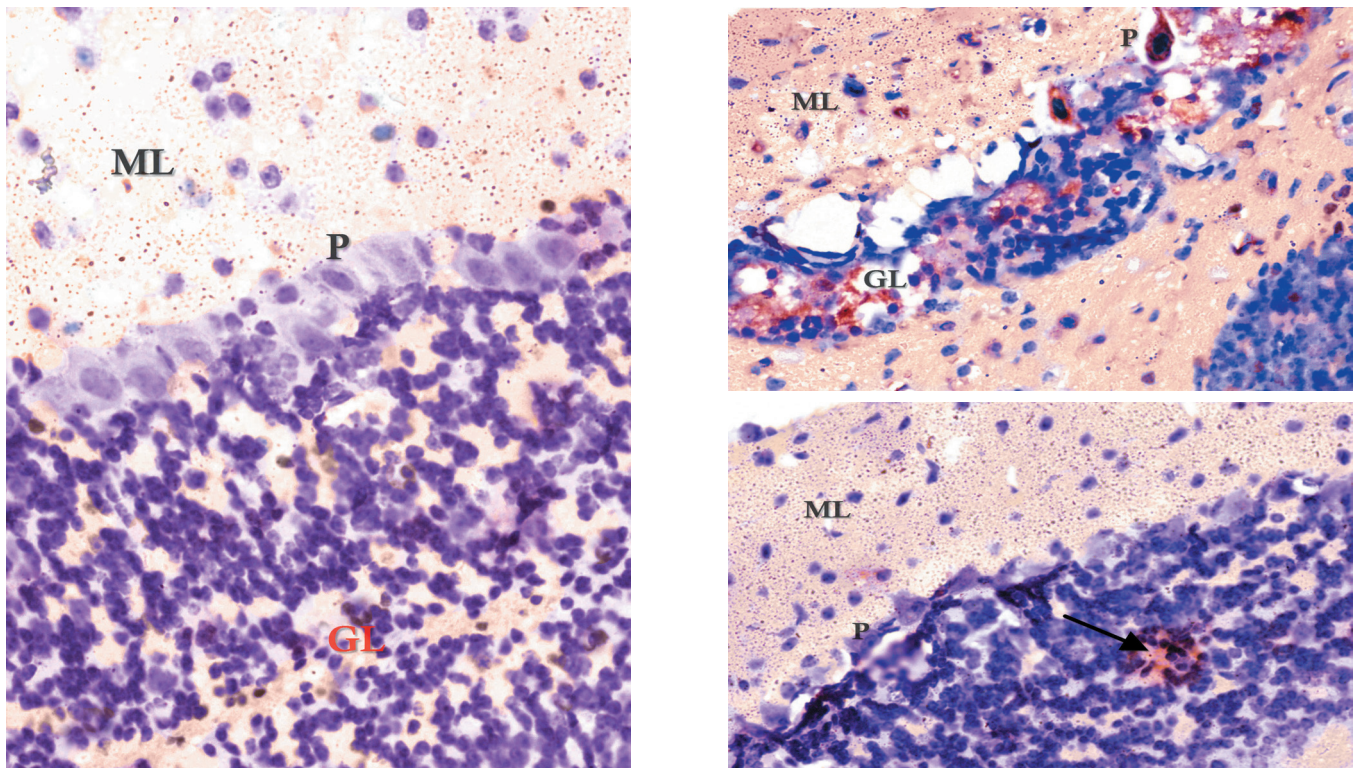


**Fig.14:** Immunohistochemical staining for the iNOS in the cerebellum of: a) an adult control mouse showing slight iNOS immunoreactivity in the molecular layer (ML) and granular layer (GL). Purkinje cell bodies (P) are non-immunoreactive. b) an adult mouse of the TiO<sub>2</sub> nanoparticles group showing strong immunoreaction in Purkinje cells cytoplasm (P). Granular cell layer (GL) shows moderate reaction in some areas (arrow) while the molecular layer (ML) shows mild immunoreactivity. c) an adult mouse of the TiO<sub>2</sub> nanoparticles + WS root extract group showing mild iNOS immunoreactivity in the molecular layer (ML) and in few areas of granular layer (arrow). Purkinje cells (P) are non-immunoreactive. iNOS, × 400

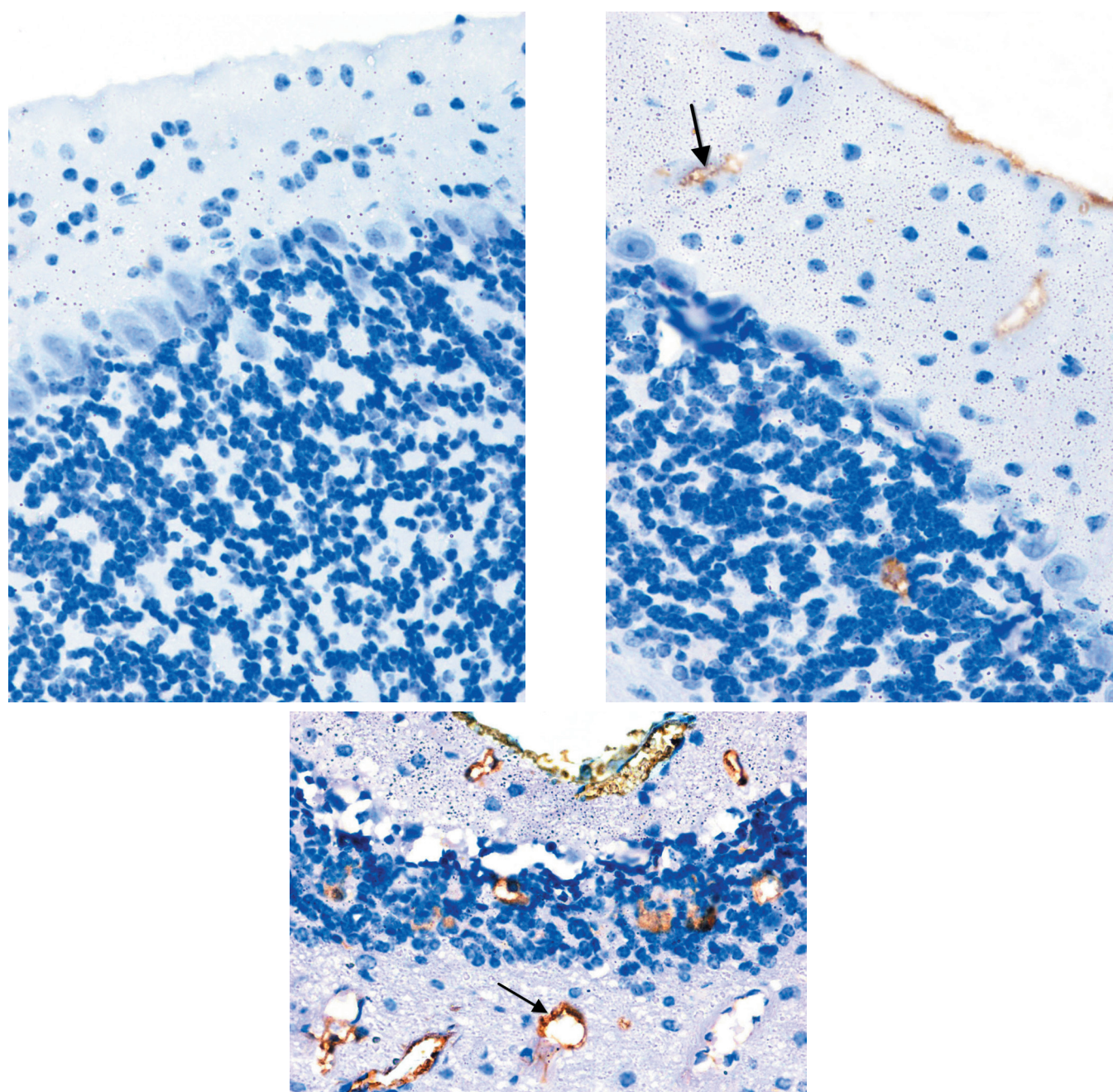


**Fig.15:** Immunohistochemical staining for the eNOS in the cerebellum of: a) an adult control mouse showing negative reaction in the capillary endothelial cells. b) an adult mouse of the TiO<sub>2</sub> nanoparticles group showing strong positive reaction in the capillary endothelial cells (arrow). c) an adult mouse of the TiO<sub>2</sub> nanoparticles + WS root extract group showing mild positive reaction in the capillary endothelial cells (arrow). eNOS, × 400

## DISCUSSION

TiO<sub>2</sub> nanoparticles have been shown to cause several pathological effects on many organs such as the kidneys, liver<sup>[24]</sup>, respiratory system<sup>[25]</sup> and reproductive system<sup>[26]</sup>.

In the present study administration of TiO<sub>2</sub> nanoparticles caused marked structural changes and disorganization in all layers of the cerebellum. Purkinje neurons were disappeared completely in many areas leaving empty spaces while in other areas they exhibited multilayer accumulation. Similar observations were found by<sup>[27]</sup> in Sodium Fluoride exposed rats who explained this finding on the basis of distal axonal neuronal degeneration.

In the current study, examination of the TiO<sub>2</sub> nanoparticles group showed that many Purkinje cells lost their pyriform shape. Most of them were shrunken with eosinophilic cytoplasm. Their nuclei were dark pyknotic or fragmented with karyolytic changes. They were surrounded with perineural spaces with accumulation of numerous glia around some of them. Vacuolation of all the layers of the cerebellar cortex were detected. The granular layer was scanty and dispersed with many cells having small dark eccentric nuclei and an eosinophilic cytoplasm.

Degeneration of cells was noticed in molecular layer, in Purkinje cell layer and in granular cell layer and vacuolization in white matter in TiO<sub>2</sub> nanoparticles exposed

cerebella of pregnant female rats and their offsprings<sup>[28]</sup>.

TiO<sub>2</sub> nanoparticles have been reported to produce condensed chromatin, fragmented nuclei, caspase activation and eventually apoptosis<sup>[29]</sup>. Nuclear shrinkage and chromatin condensation was observed in the neurons of the mouse hippocampus after treatment with TiO<sub>2</sub> nanoparticles<sup>[30]</sup>.

The appearance of eosinophilic cytoplasm and dark pyknotic or fragmented nuclei might reflect a certain phase of apoptosis<sup>[31]</sup> or might be ischemic due to the abnormalities in the capillary wall of the cerebellar cortex and thus affecting the structure of the blood-brain barrier<sup>[32]</sup>.

Oxidative stress plays a critical role in the mechanism of the toxicity induced by nanoparticles<sup>[33]</sup>. TiO<sub>2</sub> nanoparticles have also been shown to produce free radicals leading to the cell toxicity<sup>[34]</sup>. TiO<sub>2</sub> nanoparticles induced oxidative DNA damage, lipid peroxidation and increased hydrogen peroxide and nitric oxide production in human bronchial epithelial cells<sup>[35]</sup>. Moreover, TiO<sub>2</sub> nanoparticles can cause direct cell toxicity as they can enter the human body and interact with cells and its components, as proteins and lipids, affecting the cellular functions<sup>[36]</sup>.

In the current study, decreased Nissl granules was detected in the perikarya of Purkinje cells in the TiO<sub>2</sub> nanoparticles group. The decreased Nissl substance staining may be due to chromatolysis. Chromatolysis is the dissolution of the the Nissl bodies in the cell body of a neuron. It is an induced response of the cell usually triggered by either trauma or toxicity to the cell or cell exhaustion. This results in the loss of function of the protein synthesizing ability of the neurons. As, the protein is the working molecules of the cells, this may ultimately result in death of the cells<sup>[37]</sup>.

The current study revealed decrease in nNOS immunoexpression in TiO<sub>2</sub> nanoparticles group. A decrease in nNOS immunoreactivity suggests that oxidative stress affected the function of this enzyme<sup>[38]</sup>.

In the present study, the distribution of iNOS immunoreactivity in TiO<sub>2</sub> nanoparticles group detected was similar to<sup>[39]</sup> who reported that it means increased level of NO. It is stated that NO role is dependent on its concentration. At a low concentrations, NO has been included mainly in neurotransmission and vasodilatation. However, at higher concentrations, it is neurotoxic<sup>[40]</sup>.

The current study indicated statistically highly significant reduction ( $p < 0.01$ ) in the Purkinje cell number of the TiO<sub>2</sub> nanoparticles group in comparison to the control group. This great reduction gave obvious evidence about the marked deleterious effect of the TiO<sub>2</sub> nanoparticles on the Purkinje neurons.

There was an obvious dispersed arrangement of neurons in the hippocampal CA1 region after TiO<sub>2</sub> nanoparticles exposure. Furthermore, the investigation of cell numbers in the stratum pyramidale of the CA1 region indicated an

extreme neuronal loss up to 30% cell loss in female mice subjected to nasal instillation with TiO<sub>2</sub> nanoparticles<sup>[6]</sup>.

Many Bergmann astrocytes and glial cells were detected. That was confirmed by the statistical results as there was a significant increase in the number of GFAP-positive astrocytes of TiO<sub>2</sub> nanoparticles group as compared with the control groups.

The intranasal instilled TiO<sub>2</sub> nanoparticles caused increased GFAP-positive astrocytes in the molecular layer of the hippocampus<sup>[6]</sup>.

The increased glial cells, known as reactive gliosis, might be a common response to any brain insult. Following any brain injury; the glial cells get activated, increase in their cell population and secrete an inflammatory cytokines. These changes lead to positive and negative outcomes. Positively they protect neural parenchyma against ischemia, inflammation and neurodegeneration. Unfortunately glial cells secrete inflammatory cytokines and free radicals which cause neuronal damage<sup>[41]</sup>.

In the current study, many vascular changes appeared in the form of dilatation and congestion of blood vessels, exudation and hemorrhage in TiO<sub>2</sub> nanoparticles group.

Inflammation is suggested to be a possible mechanism to explain nanoparticles neurotoxicity<sup>[42]</sup>. It is suggested that neuroinflammation is involved as TiO<sub>2</sub> nanoparticles -induced changes in cytokine expression in mouse hippocampus<sup>[43]</sup>.

In the current study, TiO<sub>2</sub> nanoparticles group showed strong positive eNOS immunoreactivity in the capillary endothelial cells. The increased formation of NO by eNOS in the endothelial cells may indicate a protective mechanism of vasodilation following ischemic conditions<sup>[44]</sup>. The intravenous injection of silica NPs to mice can cause fatality due to the obstruction in the vasculature<sup>[45]</sup>.

In the present study, cerebella of TiO<sub>2</sub> nanoparticles + WS root extract group showed apparently normal histological structure in many areas. Few areas showed few apoptotic cells and few vacuolation. Cresyl fast violet stain revealed slight increase in Nissl granules in Purkinje cells as compared to the TiO<sub>2</sub> nanoparticles group. WS significantly increases the Purkinje cell count in the combined TiO<sub>2</sub> nanoparticles + WS root extract group as compared to the TiO<sub>2</sub> nanoparticles group.

In the present study the TiO<sub>2</sub> nanoparticles + WS root extract group showed improvement in nNOS immunoreactivity in molecular, granular layer and Purkinje cell layers. There was mild iNOS immunoreactivity in the molecular layer and in few areas of granular layer while Purkinje cells are non immunoreactive. Also the capillary endothelial cells showed mild positive eNOS immunoreactivity. All these findings were almost similar to the control group.

Extracts and isolated compounds have shown broad spectrum of pharmacological activities such as anti-inflammatory<sup>[46]</sup>, immunomodulation<sup>[47]</sup>, antioxidant<sup>[15]</sup> and antibacterial<sup>[48]</sup>.

WS could reverse lipid peroxidation and damage to cells. It neutralizes the free radical formation as it contains active ingredients as withanoloids<sup>[49]</sup>.

Administration of WF was found to increase superoxide dismutase, catalase and glutathione peroxidase activity in rat brain frontal cortex and striatum<sup>[15]</sup>.

WS had been shown to antagonize the DNA damage and oxidative stress induced by lead in bone marrow cells of mice<sup>[50]</sup>.

In the current study, the statistical results proven high significant decrease in the number of GFAP-positive astrocytes of TiO<sub>2</sub> nanoparticles + WS root extract group as compared with the TiO<sub>2</sub> nanoparticles group.

WS was able to revert scopolamine induced changes in GFAP expression in the glial cell of mice brain<sup>[51]</sup>.

## CONCLUSION

The exposure to TiO<sub>2</sub> nanoparticles induced major numerical and structural changes in cerebella in the albino mice and administration of the natural safe hydromethanolic root extract of WS can ameliorate these changes.

## REFERENCES

1. Warheit, D.B., Webb, T.R., Reed, K.L., Frerichs, S. and Sayes, C.M. (2007). Pulmonary toxicity study in rats with three forms of ultrafine-TiO<sub>2</sub> particles: differential responses related to surface properties. *Toxicology*; 230(1):90-104.
2. Zhao, J. and Castranova, V. (2011). Toxicology of nanomaterials used in nanomedicine. *Toxicol. J Toxicol Environ Health B Crit Rev*; 14(8):593-632.
3. Shukla, R.K., Sharma, V., Pandey, A.K., Singh, S., Sultana, S. and Dhawan, A. (2011). ROS mediated genotoxicity induced by titanium dioxide nanoparticles in human epidermal cells. *Toxicol In Vitro*; 25:231-241.
4. EL- Sharkawy, N.I.; Hamza, S.M. and Abou-Zeid, .H. (2010). Toxic Impact of Titanium Dioxide (TiO<sub>2</sub>) In Male Albino Rats with Special Reference to its Effect on Reproductive System. *Journal of American Science*; 6(11): 865-872.
5. Marquis, B.J., Love, S.A., Braun, K.L. and Haynes, C.L. (2009). Analytical methods to assess nanoparticle toxicity. *Analyst*; 134(3):425-439.
6. Wang, J., Liu, Y., Jiao, F., Lao, F., Li, W., Gu, Y., Li, Y., Ge, C., Zhou, G., Li, B., Zhao, Y., Chai, Z. and Chen, C. (2008). Time-dependent translocation and potential impairment on central nervous system by intranasally instilled TiO<sub>2</sub> nanoparticles. *Toxicology*; 254(1-2):82-90.
7. Ma, L., Liu, J., Li, N., Wang, J., Duan, Y., Yan, J., Liu, H., Wang, H. and Hong, F. (2010). Oxidative stress in the brain of mice caused by translocated nanoparticulate TiO<sub>2</sub> delivered to the abdominal cavity. *Biomaterials*; 31(1):99-105.
8. Forstermann, U., Gorsky, L.D., Pollock, J.S., Schmidt, H.H., Heller, M. and Murad, F. (1990). Regional distribution of EDRF/NO-synthesizing enzyme(s) in rat brain. *Biochem Biophys Res Commun.*; 168:727-732.
9. Lopez, I.A., Acuna, D., Beltran-Parrazal, L., Lopez, I.E., Amarnani, A., Cortes, M. and Edmond, J. (2009). Evidence for oxidative stress in the developing cerebellum of the rat after chronic mild carbon monoxide exposure (0.0025% in air). *BMC Neurosci.*; 2009: 10: 53.
10. Kiernan, J. A. (2009). *BARR'S The Human Nervous System: An anatomical viewpoint*, 9th Ed. Lippincott Williams and Wilkins; pp. 158- 171.
11. Simko, M. and Mattsson, M.O. (2010). Risks from accidental exposures to engineered nanoparticles and neurological health effects: A critical review. *Part Fibre Toxicol.*; 21;7:42.
12. Modak, M., Dixit, P., Londhe, J., Ghaskadbi, S. and Devasagayam T. P. (2007). "Indian herbs and herbal drugs used for the treatment of diabetes," *J Clin Biochem Nutr.*; 40 (3):163-173.
13. Kokate, C., Purohit, A. P. and Gokhale, S.B. (1996): "Pharmacognosy", 4th edition, Nirali Prakashan, Pune; pp. 624-629.
14. Gupta, G. L. and Rana, A.C. (2007). "Withania somnifera (Ashwagandha): a review," *Pharmacognosy Reviews*, ( 1); pp. 129-136.
15. Bhattacharya, A., Ghosal, S. and Bhattacharya, S.K. (2001). Anti-oxidant effect of Withania somnifera gly-cowithanolides in chronic foot-shock stress-induced perturbations of oxidative free radical scavenging enzymes and lipid peroxidation in rat frontal cortex and striatum. *J Ethnopharmacol.*; 74(1):1-6.
16. Manjunath, M.J. and Muralidhara (2013). Effect of Withania somnifera Supplementation on rotenone-induced oxidative damage in cerebellum and striatum of the male mice brain. *Cent Nerv Syst Agents Med Chem.* ; 13: 43-56.
17. Sriranjini, S.J., Pal, P.K., Devidas, K.V. and Ganpathy, S. (2009). Improvement of balance in progressive degenerative cerebellar ataxias after Ayurvedic therapy: a preliminary report. *Neurol, India.*; 57(2):166-171.
18. Sharma, S., Sharma, V., Pracheta and Sharma S. (2011). Therapeutic potential of hydromethanolic root extract of withania somnifera on neurological parameters in swiss albino mice subjected to lead nitrate. *International Journal of Current*

- Pharmaceutical Research.; 3, ( 2):52-56
19. Li, N., Ma, L., Wang, J., Zheng, L., Liu, J., Duan, Y., Liu, H., Zhao, X., Wang, S., Wang, H., Hong, F. and Xie, Y. (2010). Interaction between nano-anatase TiO<sub>2</sub> and liver DNA from mice in vivo. *Nanoscale Res Lett.*;5(1):108-115.
  20. Attia, H.F., Soliman, M. M., Abdel-Rahman, G. H., Nassan, M.A., Ismail, S.A., Farouk, M. and Solcan, C. (2013). Hepatoprotective effect of n-acetylcystiene on the toxic hazards of titanium dioxide nanoparticles. *American Journal of Pharmacology and Toxicology*; 8 (4): 141-147.
  21. Bancroft, J.D. and Gamble, M. (2002). "Theory and Practice of Histological Techniques". 5th ed. New York: Churchill Livingstone; pp. 593-620.
  22. Cattoretti, G., Pileri, S., Parravicini, C., Becker, M.H., Poggi, S., Bifulco, C., Key, G., D'Amato, L., Sabbatini, E. and Feudale, E. (1993). Antigen unmasking on formalinixed, paraffinembedded tissue sections. *J. Pathol.*; 171(2): 83-98.
  23. Doulazmi, M., Frederic, F., Lemaigre-Dubreuil, Y., Hadj-Sahraoui, N., Delhaye-Bouchaud, N. and Mariani, J. (1999). Cerebellar Purkinje cell loss during life span of the heterozygous staggerer mouse (Rora+)/Rora(sg)) is gender-related. *J Comp Neurol.*;411(2):267-73.
  24. Liang, G., Pu, Y., Yin, L., Liu, R., Ye, B., Su, Y. and Li, Y. (2009). "Influence of different sizes of titanium dioxide nanoparticles on hepatic and renal functions in rats with correlation to oxidative stress," *J Toxicol Environ Health A.*;72 (11-12):740-745.
  25. Moon, C., Park, H.J., Choi, Y.H., Park, E.M., Castranova, V. and Kang, J.L.(2010). "Pulmonary inflammation after intraperitoneal administration of ultrafine titanium dioxide (TiO<sub>2</sub>) at rest or in lungs primed with lipopolysaccharide," *J Toxicol Environ Health A.*;73(5):396-409.
  26. Guo, L.L., Liu, X.H., Qin, D.X., Gao, L., Zhang, H.M., Liu, J.Y. and Cui, Y.G. (2009). "Effects of nanosized titanium dioxide on the reproductive system of male mice," *Zhonghua Nan Ke Xue*;15(6):517-522.
  27. Affi, O.K. (2009). Effect of Sodium Fluoride on the Cerebellar Cortex of Adult Albino Rats and the Possible Protective Role of Vitamin B6: A Light and Electron Microscopic Study. *Egypt. J. Histol.*; 32( 2): 358-367.
  28. El Ghareeb, A., Hamdi, H., El Bakry, A. and Abo Hmela, H. (2015). Teratogenic Effects of the Titanium Dioxide Nanoparticles on the Pregnant Female Rats And Their Off Springs. *RJPBCS.*; 6(2):510-523.
  29. Park, E.J., Yi, J., Chung, K.H., Ryu, D.Y., Choi, J. and Park, K. (2008). Oxidative stress and apoptosis induced by titanium dioxide nanoparticles in cultured BEAS-2B cells. *Toxicol Lett.*;180(3):222-229.
  30. Hu, R., Zheng, L., Zhang, T., Gao, G., Cui, Y., Cheng, Z., Cheng, J., Hong, M., Tang, M. and Hong, F. (2011) . Molecular mechanism of hippocampal apoptosis of mice following exposure to titanium dioxide nanoparticles. *J Hazard Mater*;191(1-3):32-40.
  31. Ratan, R.R., Murphy, T.H. and Baraban, J.M. (1994). Oxidative stress induces apoptosis in embryonic cortical neurons. *J.Neurochem.*; 62(1):376-379.
  32. Sobaniec-Lotowska, M.E. (2001). Ultrastructure of Purkinje cell perikarya and their dendritic processes in the rat cerebellar cortex in experimental encephalopathy induced by chronic application of valproate. *Int.J.Exp.Pathol.*; 82(6):337-348.
  33. Rushton, E.K., Jiang, J., Leonard, S.S., Eberly, S., Castranova, V., Biswas, P., Elder, A., Han, X., Gelein, R., Finkelstein, J. and Oberdorster, G. (2010): Concept of assessing nanoparticle hazards considering nanoparticle dose-metric and chemical/biological response metrics. *J. Toxicol. Environ. Health A.*; 73(5):445–461.
  34. Barnard, A.S. (2010). One-to-one comparison of sunscreen efficacy, aesthetics and potential nanotoxicity. *Nat Nanotechnol.*;5(4):271-274.
  35. Guur, J. R., Wang, A. S., Chen C. H. and Jan, K. Y. (2005) Ultrafine titanium dioxide particles in the absence of photoactivation can induce oxidative damage to human bronchial epithelial cells. *Toxicology*; 213(1-2):66-73.
  36. Nel, A., Xia, T., Madler, L. and Li, N. (2006). Toxic potential of materials at the nanolevel. *Science*; 311: 622–627.
  37. Snell, R. S. (2010). *Clinical Neuroanatomy*. Lippincott Williams Wilkins, Baltimore, Md, USA, 7<sup>th</sup> edition. Pp. 36-38.
  38. Vaccari, A., Ruiu, S., Saba, P., Fà, M., Cagiano, R., Coluccia A., Mereu, G., Steardo, L., Tattoli, M., Trabace, L. and Cuomo, V. (2001). Prenatal low-level exposure to CO alters postnatal development of hippocampal nitric oxide synthase and haem-oxygenase activities in rats. *Int J Neuropsychopharmacol.*;4(3):219-22.
  39. Chung, Y.H., Shin, C.M.,Joo, K.M., Kim, M.J. and Cha, C.L. (2002). Immunohistochemical study on the distribution of nitrotyrosine and neuronal nitric

- oxide synthase in aged rat cerebellum. *Brain Res.*; 951 (2): 316-321.
40. Jana, M., Liu, X., Koka, S., Ghosh, S., Petro, T.M. and Pahan, K. (2001). Ligation of CD40 stimulates the induction of nitric-oxide synthase in microglial cells. *J. Biol. Chem.*; 276(48):44527-44533.
  41. Verkhratsky, A., Sofroniew, M.V., Messing, A., deLanerolle, N.C., Rempe, D., Rodríguez, J.J. and Nedergaard, M. (2012). Neurological diseases as primary gliopathies: a reassessment of neurocentrism. *ASN Neuro.*; 5:4(3), e00082.
  42. Sayes, C.M., Wahi, R., Kurian, P.A., Liu, Y., West, J.L., Ausman, K.D., Warheit, D.B. and Colvin, V.L. (2006). Correlating nanoscale titania structure with toxicity: a cytotoxicity and inflammatory response study with human dermal fibroblasts and human lung epithelial cells. *Toxicol Sci.*; 92(1):174–185
  43. Ze, Y., Sheng, L., Zhao, X., Hong, J., Ze, X., Yu, X., Pan, X., Lin, A., Zhao, Y., Zhang, C., Zhou, Q., Wang, L. and Hong, F. (2014). TiO<sub>2</sub> Nanoparticles Induced Hippocampal Neuroinflammation in Mice. *PLoS ONE*; 9(3): e92230.
  44. Wei, G., Dawson, V.L. and Zweier, J.L. (1999). Role of neuronal and endothelial nitric oxide synthase in nitric oxide generation in the brain following cerebral ischemia. *Biochim Biophys Acta.*; 20;1455(1):23-34.
  45. Yu, T., Greish, K., McGill, L. D., Ray, A. and Ghandehari, H. (2012). Influence of geometry, porosity and surface characteristics of silica nanoparticles on acute toxicity: their vasculature effect and tolerance threshold. *ACS Nano.*; 6:2289-2301.
  46. Gupta, A. and Singh, S. (2014). Evaluation of anti-inflammatory effect of *Withania somnifera* root on collagen-induced arthritis in rats. *Pharm Biol.*;52(3):308-320.
  47. Rasool, M. and Varalakshmi, P. (2006). Immunomodulatory role of *Withania somnifera* root powder on experimental induced inflammation: An in vivo and in vitro study. *Vascul Pharmacol.*; 44(6):406-410.
  48. Owais, M., Sharad, K.S., Shehbaz, A. and Saleemuddin, M. (2005). Antibacterial efficacy of *Withania somnifera* (ashwagandha) an indigenous medicinal plant against experimental murine salmonellosis. *Phytomedicine*;12(3):229-235.
  49. Dhuley, J.N. (2000). Adaptogenic and cardioprotective action of ashwagandha in rats and frogs. *J Ethnopharmacol.*;70(1):57-63.
  50. Khanam, S. and Devi, K. (2005). Effect of *Withania somnifera* root extract on lead-induced DNA damage. *International Journal of Food, Agriculture and Environment*; 3: 31–33.
  51. Konar, A., Shah, N., Singh, R., Saxena, N., Kaul, S.C., Wadhwa, R. and Thakur, M.K. (2011). Protective role of Ashwagandha leaf extract and its component withanone on scopolamine-induced changes in the brain and brain-derived cells. *PLoS One*;6(11):e27265.

## الملخص العربي

**التخفيف من ضرر جزيئات ثاني أكسيد التيتانيوم متناهية الصغر على مخيخ الفئران البيضاء البالغة بواسطة مستخرج هيدروميثانولي من جذور ويثانيا سومنيفيرا**

**نرمين محمد فهيم و أمجد جابر السعيد  
قسم التشريح و الأجنة, كلية الطب, جامعة عين شمس**

**المقدمة:** تشكل جزيئات ثاني أكسيد التيتانيوم متناهية الصغر مخاطر محتملة على صحة الإنسان. حيث أنها قادرة على الدخول للدماغ و الوصول إلي قشرة المخ و المخيخ. ويثانيا سومنيفيرا قادرة علي حماية المخيخ من الإصابة بالروتينون.

**الهدف من الدراسة:** دراسة الاثار المترتبة من تناول جزيئات ثاني أكسيد التيتانيوم متناهية الصغر بالفم علي مخيخ الفئران البيضاء و الدور الوقائي لمستخرج هيدروميثانولي من جذور من ويثانيا سومنيفيرا.

**المواد وطرق البحث:** تم تقسيم خمسة وسبعون من ذكور الفئران البيضاء البالغة إلى خمس مجموعات المجموعة 1 (الضابطة)، المجموعة 2 (مجموعة السنط)، مجموعة 3 (هيدروميثانوليك الجذر المستخرج من ويثانيا سومنيفيرا) (500 ملغم / كغم) مرة واحدة يوميا، مجموعة 4 (جزيئات ثاني أكسيد التيتانيوم متناهية الصغر) 150 ملغم/ كغم بالفم مذابا في السنط و المجموعة 5 (جزيئات ثاني أكسيد التيتانيوم متناهية الصغر+ مستخرج هيدروميثانولي من جذور من ويثانيا سومنيفيرا) الجرعة كما في الجرعات السابقة. تم إستخراج المخيخ من جميع الفئران بعد ستين يوما وقطعت لشرائح و تم تجهيزها للصبغ بصبغات الهيماتوكسلين و الايوسين و الكريسيل فاست البنفسجي بالإضافة لعدد من الصبغات المناعية و تم عمل تحليل إحصائي لعدد خلايا البركيني و الخلايا النجمية.

**النتائج:** عينات المجموعة الرابعة أظهرت الخلايا العصبية وجود أضرار بالغة مع وجود اثار ضمور و كانت الأنويه غامقة اللون بالإضافة إلى إنخفاض ملحوظ بحبيبات نسل. و قد وجد فراغات بجميع طبقات قشرة المخيخ. كما كانت الأوعية الدموية منتفخة و محتقنة بالدم. ووجد نقص حاد في خلايا البركيني في هذه المجموعة و لكن الخلايا النجمية زادت زيادة ملحوظة. أما الصبغة المناعية أوضحت حدوث زيادة في للإنزيم المستحث المصنع لأكسيد النتريك و كذلك في الإنزيم الطلائي المصنع لأكسيد النتريك. بينما حدث نقص في الإنزيم العصبي المصنع لأكسيد النتريك. و على الجانب الأخر أوضحت المجموعة التي تم علاجها بمستخرج هيدروميثانولي من جذور من ويثانيا سومنيفيرا تحسن في التغيرات النسيجية بالإضافة إلى عكس نتائج الإنزيم المصنع لأكسيد النتريك و عدد خلايا البركيني و الخلايا النجمية.

**الخلاصة:** ونستخلص من ذلك أن مستخرج هيدروميثانولي من جذور ويثانيا سومنيفيرا يحتوي علي مواد فعالة تؤدي إلى تقليل التغيرات النسيجية الحادثة في قشرة المخيخ بإستخدام جزيئات ثاني أكسيد التيتانيوم متناهية الصغر.